Valence band spectra of 4d and 5d silicides

1997 J. Phys.: Condens. Matter 9 9403

(http://iopscience.iop.org/0953-8984/9/43/023)

J. Phys.: Condens. Matter **9** (1997) 9403–9414. Printed in the UK PII: S0953-8984(97)84429-3

Valence band spectra of 4d and 5d silicides

Yu M Yarmoshenko†, S N Shamin†, L V Elokhina†, V E Dolgih†, E Z Kurmaev†¶, S Bartkowski‡, M Neumann‡, D L Ederer§, K Göransson‖, B Noläng‖ and I Engström‖

† Institute of Metal Physics, Russian Academy of Sciences—Ural Division, 620219 Yekaterinburg GSP-170, Russia

‡ Fachbereich der Physik, Universität Osnabrück, D-49069 Osnabrück, Germany

§ Department of Physics, Tulane University, New Orleans, LA 70188, USA

‖ Institute of Chemistry, University of Uppsala, Box 531, S-75121 Uppsala, Sweden

Received 20 May 1997

Abstract. A full study of the electronic structure of 4d and 5d silicides (RuSi, RhSi, PdSi, OsSi, IrSi, Ir_3Si_5, $IrSi_3$, PtSi) is undertaken including XPS VB and XES (Si K$\beta_{1,3}$ and Si $L_{2,3}$) measurements and LMTO band structure calculations. It is found that d bands which dominate the density of states are more localized with increasing atomic number Z of the transition metal. A strong hybridization between silicon 3p and transition metal d states occurs over the entire valence band. Si 3s states are found to be not mixed with Si 3p and nd states but Si 3d states participate in bonding and hybridize with transition metal d states. The non-bonding character of the majority of nd states is not confirmed for 4d and 5d silicides.

1. Introduction

A study of the electronic structure of transition metal silicides is of great relevance for an understanding of the interactions at metal–silicon interfaces. Among many metallic compounds, silicides have attracted attention as materials for metal–semiconductor junctions required for Schottky barriers and for ohmic contacts due to their high conductivity, high thermal stability and compatibility with Si. To better understand chemical bonding at the interface and to identify potential structural and electronic differences between bulk silicides and silicide-like phases, one must examine both bulk and interface silicides. In addition, x-ray emission spectra of reference silicides are important for the analysis of solid phase reactions at metal–silicon interfaces under heat treatment [1]. Up to now only the electronic structures of 3d transition metal silicides have been studied in detail [2–7]. Among the 4d and 5d transition metal silicides generally those with few d electrons [8] and some near-noble-metal monosilicides [9–11] have been analysed.

In the present paper a complete study of the electronic structure of specially prepared 4d and 5d near-noble-metal silcides (RuSi, RhSi, PdSi, OsSi, IrSi, Ir_3Si_5, $IrSi_3$, PtSi) was made using x-ray photoelectron spectroscopy (XPS) and x-ray emission spectroscopy (XES). XPS provides useful information on the total density of states (DOS) distribution in the valence band (VB), while XES gives the partial DOS allowed by the dipole selection rule for electron transitions. The obtained results were compared with LMTO band structure calculations for these compounds.

¶ Corresponding author. E-mail address: kurmaev@ifmlrs.uran.ru

0953-8984/97/439403+12$19.50

2. Experimental and calculation details

Binary 4d and 5d silicides were obtained by arc melting of the metals and silicon in argon atmosphere. Quoted purities of the materials used were for silicon 99.999% (Highways International) and for the metals 99.9% (Johnson–Matthey). All samples except RhSi(HT) and $IrSi_3$(LT) were annealed at 1000 °C in evacuated silica tubes for 24 h. RhSi(HT) was quenched directly from the melt, and $IrSi_3$(LT) annealed at 900 °C, under the same conditions as the other samples. Phase identification and cell parameter determination was performed using Guinier–Hägg-type x-ray powder cameras with Cu Kα_1 radiation for all samples except the two $IrSi_3$ samples for which Cr Kα_1 was used due to extensive peak overlap. The structural data of 4d and 5d silicides are given in table 1. For more details see [12] and [20–24].

Table 1. Structural data of 4d and 5d silicides.

Compound	Structure	Space group	Cell parameters (Å)	Composition
RuSi	CsCl	$Pm3m$	$a = 2.914\,618$	$Ru_{50}Si_{50}$
RhSi (LT)	MnP	$Pnma$	$a = 5.552\,63$	$Rh_{50}Si_{50}$
			$b = 3.068\,92$	
			$c = 6.374\,04$	
RhSi (HT)	FeSi	$P2_13$	$a = 4.686\,39$	$Rh_{49}Si_{51}$
PdSi	MnP	$Pnma$	$a = 5.614\,05$	$Pd_{48}Si_{52}$
			$b = 3.386\,04$	
			$c = 6.149\,85$	
OsSi	FeSi	$P2_13$	$a = 4.724\,15$	$Os_{50}Si_{50}$
IrSi	MnP	$Pnma$	$a = 5.553\,59$	$Ir_{50}Si_{50}$
			$b = 3.218\,76$	
			$c = 6.267\,611$	
PtSi	MnP	$Pnma$	$a = 5.581\,75$	$Pt_{48}Si_{52}$
			$b = 3.596\,23$	
			$c = 5.925\,86$	
$IrSi_3$	monocl.	—	$a = 7.700\,28$	$Ir_{25}Si_{75}$
			$b = 4.377\,66$	
			$c = 6.546\,98$	
			$\beta = 91.611\,10$	
$IrSi_3$	orthorhomb.	—	$a = 7.554\,116$	$Ir_{20}Si_{80}$
			$b = 4.350\,99$	
			$c = 6.631\,716$	
Ir_3Si_5	Ir_3Si_5	$P2_1/c$	$a = 6.407\,010$	$Ir_{40}Si_{60}$
			$b = 14.1572$	
			$c = 11.5672$	
			$\beta = 116.6689$	

The XPS measurements have been carried with an ESCA spectrometer made by Physical Electronics (PHI 5600 ci). The monochromatized Al Kα radiation had an FWHM of 0.3 eV which combined with the energy resolution of the analyser (1.5% of the pass energy) provided an estimated energy resolution somewhat less than 0.35 eV for the XPS measurements of 4d and 5d silicides. The pressure in the vacuum chamber during the measurements was less than 5×10^{-9} mbar. All of the compounds studied were available in an ingot form which was suitable for cleavage in ultra-high vacuum for XPS measurements of surfaces free of contaminations. All the investigations have been performed at room temperature on the cleaved surface of ingots. Thus contaminant free surfaces with a

relatively small number of defects could be used to obtain the intrinsic properties of the samples. The XPS spectra were calibrated using Au $4f_{7/2}$ signal from an Au foil ($E_{b.e.}$(Au $4f_{7/2}$) = 84.0 eV).

Si $L_{2,3}$ x-ray emission spectra (valence 3s3d $\rightarrow$ 2p transition) excited by an electron beam were measured with an ultrasoft x-ray spectrometer [4] with a spatial resolution of 4–5 μm and energy resolution of 0.4 eV. The Si $L_{2,3}$ x-rays were produced by a 130 nA current of 4 keV electrons and were diffracted by an $N = 600$ lines mm^{-1} diffraction grating having a 2 m radius of curvature.

The Si K$\beta_{1,3}$ x-ray emission spectra (valence 3p $\rightarrow$ 1s transition) were measured with a fully focused Johan type spectrometer (energy resolution was about 2.5 eV). The x-ray tube was operated at an anode voltage of 5 keV and a current of 100 nA and the position of the sample was changed with respect to the focused electron beam for each scan to reduce sample decomposition and contamination.

The x-ray emission spectra have been adjusted to the scale of electron binding energies with respect to the Fermi level by using the XPS binding energies of the Si 2p states (see table 2). The value of the Si Kα_1 line (2p $\rightarrow$ 1s transition), $E = 1740.1$ eV, was used to calibrate Si $L_{2,3}$ and Si K$\beta_{1,3}$ XES of 4d and 5d silicides.

Table 2. Energy position of the spectral maximum of Si $L_{2,3}$ (XES), Si K$\beta_{1,3}$ (XES) and binding energies of Si 2s (XPS) and Si 2p (XPS) core levels of 4d and 5d silicides (in eV).

Compound	Si $L_{2,3}$ (XES)	Si K$\beta_{1,3}$ (XES)	Si 2s (XPS)	Si 2p (XPS)
RuSi	90.3	1835.0	150.4	99.0
RhSi(MnP)	90.4	1834.5	150.6	99.1
RhSi(HT)	90.5	1834.8	150.6	99.3
PdSi	91.3	1834.8	150.8	99.3
OsSi	90.3	1835.5	150.7	99.3
$IrSi_3$(HT)	91.7	1836.1	150.6	99.4
$IrSi_3$(LT)	91.6	1836.1	150.9	99.4
Ir_3Si_5	90.6	1834.8	150.9	99.4
IrSi	90.3	1835.2	150.9	99.4
PtSi		1834.8		

The valence band DOSs were calculated using the linear muffin-tin orbital method in the atomic-sphere approximation (LMTO–ASA) [13, 14]. The core electrons were treated separately in a fully relativistic program and kept frozen in the band structure calculations. Relativistic effects were included except spin–orbit coupling for the valence electrons. The local density approximation for exchange and correlation with the potential of von Barth and Hedin [15] was used. For silicides having the FeSi-type structures 506 mesh points were used in the irreducible 1/24 first Brillouin zone (BZ), while for silicides having the CsCl structure 680 mesh points were used in the irreducible 1/48 first BZ, and finally silicides with the MnP-type structure required 252 mesh points in the irreducible 1/8 first BZ. Plots of the density of states (DOS) against energy were constructed from calculated eigenvalues by the tetrahedron integration method at the calculated equilibrium volumes. These volumes differ by less than 5% from the experimental volumes. s, p and d basis functions were used for all atomic spheres. The exact amount of calculated silicon d states will depend strongly on the choice of atomic sphere size since these electrons are concentrated in the outer parts

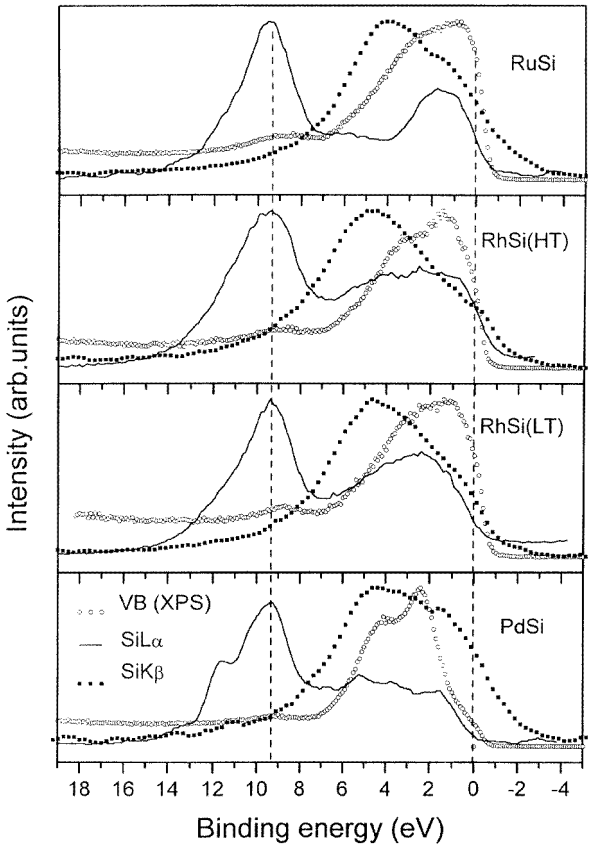

Figure 1. Comparison of Si K$\beta_{1,3}$ and Si $L_{2,3}$ XES and XPS VB for 4d silicides.

of the Si atomic spheres†. The selected ratios between metal and silicon atomic sphere radii range from 1.02 (RuSi) to 1.10 (PtSi), following the trend in metallic radii for the elements. This gives approximately the same potential at the surface of the metal and silicon spheres respectively.

3. Results and discussion

The x-ray emission and photoelectron spectra of 4d and 5d silicides are presented in figures 1 and 2 and energies of features in the spectra are given in table 2. In accordance with dipole selection rules Si $L_{2,3}$ and Si K$\beta_{1,3}$ XES probe Si 3s3d and Si 3p partial DOS in the valence band, respectively. The intensities of Si $L_{2,3}$ and Si K$\beta_{1,3}$ XES and XPS VB are not given in absolute units, and therefore cannot be used to estimate the ratio of the contribution of Si 3p to Si 3s3d and transition metal *n*d states. The results of LMTO band structure calculations given in figures 3 and 4 can be used for this comparison. According to [16] the

† The DOS features labelled as silicon d electrons have their origins in the outer parts of the metal d shells. Calculations performed for IrSi show that the total d DOS can be reproduced if silicon d states are removed from the calculations, provided the metal spheres are allowed to expand so as to contain the outermost d-electron density (atomic sphere radius ratio $r_{Ir}/r_{Si} \simeq 1.4$).

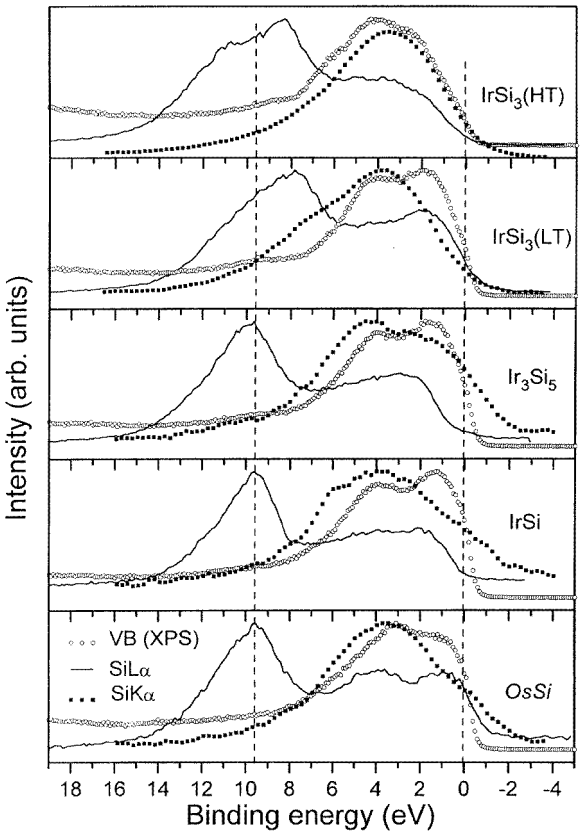

Figure 2. Comparison of Si K$\beta_{1,3}$ and Si $L_{2,3}$ XES and XPS VB for 5d silicides.

atomic photoionization cross sections at the Al Kα excitation energy (1.476 keV) for Ru 4d, Rh 4d, Pd 4d, Os 5d and Ir 5d subshell electrons are nearly two orders of magnitude larger than the Si 3p and Si 3s subshell photoionization cross sections. This large difference in the cross sections leads us to suggest that the XPS valence band data of the 4d and 5d silicides provide information mainly about the transition metal *n*d-state distribution in the valence band. In figure 1 the Si $L_{2,3}$ XES spectra (line), the Si K$\beta_{1,3}$ XES (solid squares) and the x-ray photoelectron valence band spectra (XPS VB) (open circles) are compared. We infer that the Si valence states of 3s symmetry are concentrated at the bottom of the valence band (7–13 eV below E_f because of the dipole selection of states of s symmetry in the Si $L_{2,3}$ XES spectra. The valence states of s symmetry show up weakly in the XPS VB spectra because the VB states of 3s symmetry have a very small photoionization cross section. At intermediate energies between 2 eV and 7 eV below E_f we infer the presence of bands with 3p symmetry from the intensity profile of the Si K$\beta_{1,3}$ emission band which emphasizes states of p symmetry. Overlap of the Si K$\beta_{1,3}$ XES with XPS VB spectra suggests the hybridization of the Si 3p electrons with the transition metal 4d electrons. In the vicinity of the Fermi level (in the range of 0–2 eV) the distribution of electronic states is more complicated. On the one hand, 4d states prevail in this region (at least for RuSi and RhSi). On the other hand, the Si 3p and Si 3s(3d) electrons also make an essential contribution to the DOS.

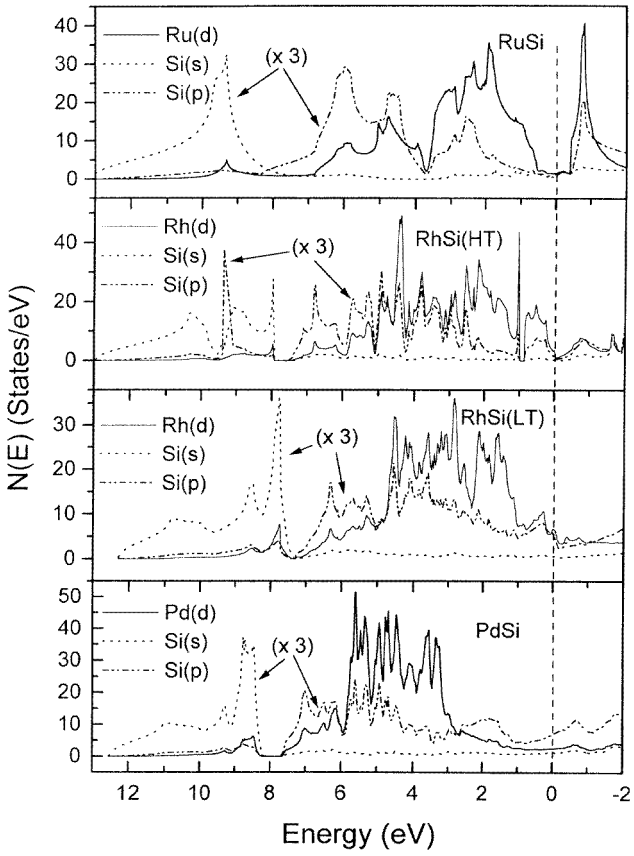

Figure 3. Results of LMTO–ASA band structure calculations for 4d silicides.

We have not detected great differences between experimental spectra of RhSi(HT) and RhSi(LT) phases shown in figure 1 except some broadening of the peaks centred at 9.3 eV binding energy of Si $L_{2,3}$ XES of RhSi(HT) (compared to similar spectrum of RhSi(LT)). This broadening can be explained by increasing number of Si neighbours of the Si atom from four to six. The Si–Si interatomic distances are similar in both cases (as noted in table 3).

Let us next consider the variation of the 4d DOS near the Fermi level for the set of silicides RuSi–RhSi–PdSi. The variation of the XPS spectra of these compounds, shown in figure 1, provides evidence that the XPS VB intensity maximum is very close to the Fermi energy for RuSi, at an intermediate value for RhSi and at a binding energy of a few eV for PdSi. Thus the contribution of 4d states to the total DOS at the Fermi edge is decreasing steadily from RuSi to RhSi and PdSi. At the same time the intensity maximum of XPS VB shifts from the Fermi energy to binding energies of about 3 eV. We suggest this is due to the localization of the 4d states as a function of the atomic number Z of the 4d metal. This shift is about 1 eV for RhSi in respect to that of RuSi and increases to about 3 eV for PdSi. These conclusions about the electronic structure of 4d monosilicides which have been extracted from XPS and XES data are in a good accordance with our band structure calculations of the same compounds which are shown in figure 3. It is seen that a strong

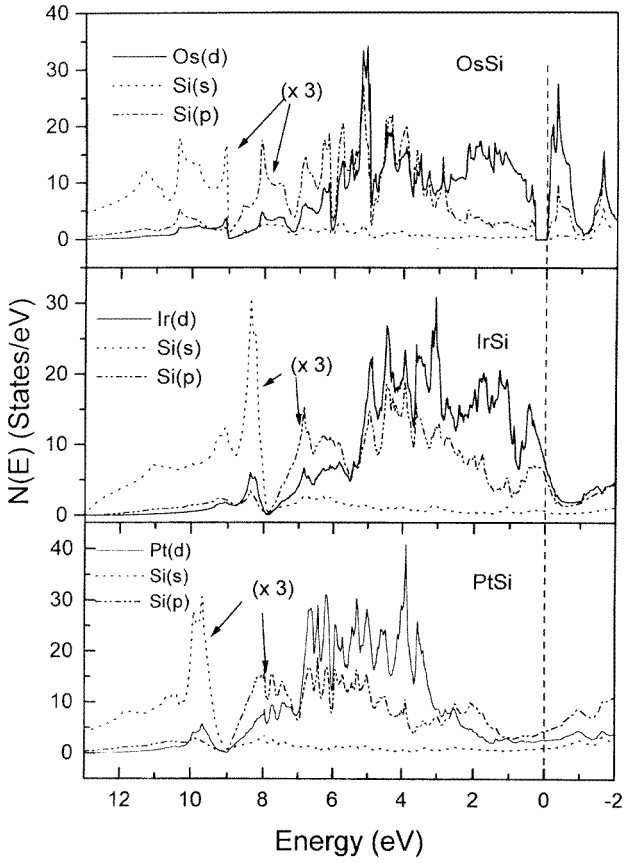

Figure 4. Results of LMTO–ASA band structure calculations for 5d silicides.

hybridization between transition metal *n*d states and silicon 3p states takes place over the whole valence band and the centre of gravity of Si 3p states is shifted in PdSi to a higher binding energy with respect to that of RhSi following a similar shift of the d band.

We can conclude from similar analysis of the XES:XPS spectra of the 5d silicides (in figure 2)† that the Si 3s-like band has a binding energy of approximately 10 eV, the Si 3p DOS extends over an energy range of 1–8 eV binding energy and finally the changing intensity and energy position of the XPS VB data reflect the filling of the partial DOS with 5d symmetry. The results of LMTO band structure calculations of 5d silicides (figure 4) are consistent with our interpretation of the experiments. As in the case of 4d silicides, a strong transition metal 5d–Si 3p hybridization is found for 5d silicides and the centre of gravity of Si 3p states is shifted to a higher binding energy in PtSi with respect to that in IrSi. The overall agreement of theory and experiment can be illustrated by comparing the Si K$\beta_{1,3}$ XES of 4d and 5d silicides with the calculated Si 3p DOS in figure 5 (shown as the line) that has been broadened to include instrumental distortion in figure 5.

Comparing the experiments with theory we observe a pronounced peak near the Fermi edge in the Si $L_{2,3}$ spectra that is not seen in the calculated silicon density of states with either s or p symmetry. We conclude that these additional features near the Fermi energy are

† For PtSi we could not measure XPS VB with a good accuracy because of oxidation of the surface.

Table 3. Coordination numbers (CN) and average distances (AD) of Me–Me, Me–Si and Si–Si bonds (in Å) of 4d and 5d silicides obtained from [11] and [16–20].

Compound	CN Me–Me	AD Me–Me	CN Me–Si	AD Me–Si	CN Si–Si	AD Si–Si	Ref.
RuSi	6	2.91	8	2.52	6	2.91	[11]
RhSi	2	2.85	2	2.38	2	2.66	[11]
(LT)	2	2.99	1	2.44	2	3.07	
	2	3.07	2	2.50			
			1	2.51			
RhSi	6	2.87	3	2.45	6	2.90	[16]
(HT)			1	2.47			
			3	2.57			
PdSi	4	2.90	1	2.45	2	2.76	[17]
			2	2.46			
			1	2.54			
			2	2.57			
OsSi	6	2.90	1	2.35	6	2.94	[11]
			3	2.41			
			3	2.74			
IrSi	2	2.84	2	2.34	2	2.69	[11]
	2	3.01	1	2.52			
	2	3.22	2	2.53			
			1	2.54			
PtSi	2	2.87	1	2.41	2	2.84	[18]
	2	2.90	2	2.43			
			1	2.52			
			2	2.64			
Ir_3Si_5	2.3	2.85–3.00	5.5	2.30–2.50	2.9	2.50–2.70	[19]
			1.2	2.50–2.80	0.9	2.70–2.90	
			0.5	2.80–3.10	0.4	2.90–3.10	
$IrSi_3$	6	4.16	6	2.44	2	1.97	[20]
(HT)			3	2.49	2	2.37	

due to bands formed by hybridizing Si 3d states with the transition metal 4d and 5d states. When the partial densities of states with d symmetry at the silicon site are projected out and broadened according to instrumental distortion we obtain extremely good agreement with the observed Si $L_{2,3}$ spectra. In figure 6 the Si $L_{2,3}$ spectra (dots) for the 4d and 5d silicides are compared with the calculated Si partial density of states of s + d symmetry (solid line). The silicon d-partial DOS is shown separately as the shaded area. We note the very good agreement obtained when the states with d symmetry are included in the calculation. A similar conclusion was reached for 3d monosilicides (FeSi, CoSi, NiSi) and disilicides ($FeSi_2$, $CoSi_2$, $NiSi_2$) in [4], [5] and [7]. Our measurements support the conclusion given in [7] that a p–d bonding model [19] does not provide a complete description of the electronic structure of d silicides and Si 3d–metal *n*d hybridization must be taken into account.

For the Ir–Si system a full set of binary compounds (high-temperature (HT) and low-temperature (LT) modifications of $IrSi_3$, Ir_3Si_5 and IrSi) was specially prepared (in connection with a study of solid-phase reactions at the Ir/Si interface under different heat treatments [17]). We also measured the XES and XPS spectra of these materials, shown in figures 1 and 2. XPS VBs of Ir silicides given in figure 2 definitely show that the density of states on the Fermi level is highest for IrSi and is decreasing with Ir content because of the Ir 5d shift to lower binding energy [25]. This shift can be explained by increasing

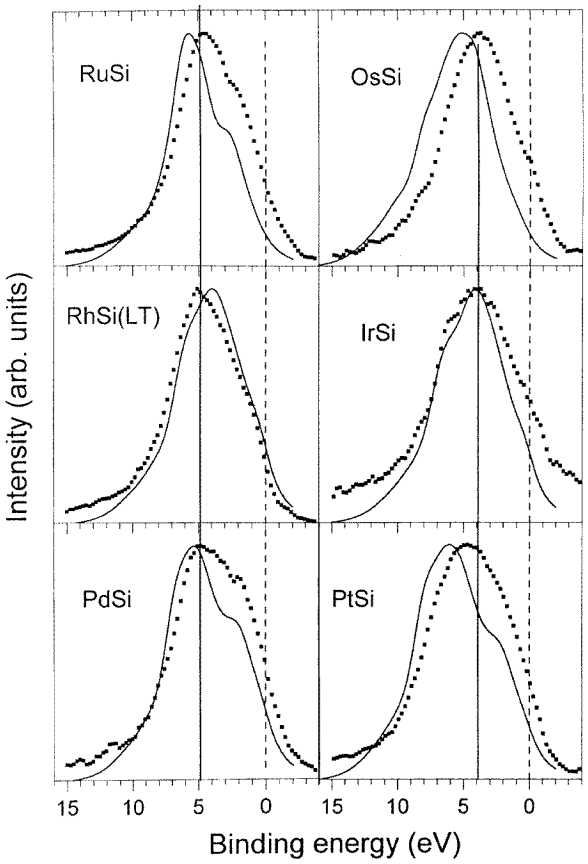

Figure 5. Comparison of Si K$\beta_{1,3}$ XES and Si 3p DOS of 4d and 5d silicides.

of silicon content per unit formula in Si-rich silicides. In this case the antibonding states are being filled and the quasigap is shifted to below E_f [11]. The greatest changes are found also for Si $L_{2,3}$ XES of IrSi and $IrSi_3$ which are shown separately for convenience in figure 7. An energy shift (about 1 eV) and some broadening and even splitting of the main intensity maximum is seen in Si $L_{2,3}$ XES of Ir binary silicides with Ir content (top dotted curve). In order to interpret the Si $L_{2,3}$ XES in silicides we need to take into account both Si–metal and the Si–Si interactions. According to structural data, an Si atom in IrSi is coordinated by only two Si atoms whereas in $IrSi_3$ it is coordinated by four Si atoms as in crystalline Si (see table 3†). This additional coordination is illustrated by comparing the Si $L_{2,3}$ spectrum of $IrSi_3$ with that of crystalline Si (the solid line in figure 7). The corresponding Si–Si bonds are shorter in $IrSi_3$ than in IrSi, thus the contribution of the Si–Si interactions increases and it is not surprising to observe that Si $L_{2,3}$ XES of $IrSi_3$ has nearly the same splitting of the main maximum as crystalline silicon (c-Si) (figure 7). According to [9] the strength of Si–Si bonding increases with decreasing distance between silicon neighbours which enhances the amount of wave-function overlap of the Si 3s states, resulting in the broadening of the Si $L_{2,3}$ XES.

† For $IrSi_3$(HT) only a very approximate structure description is given.

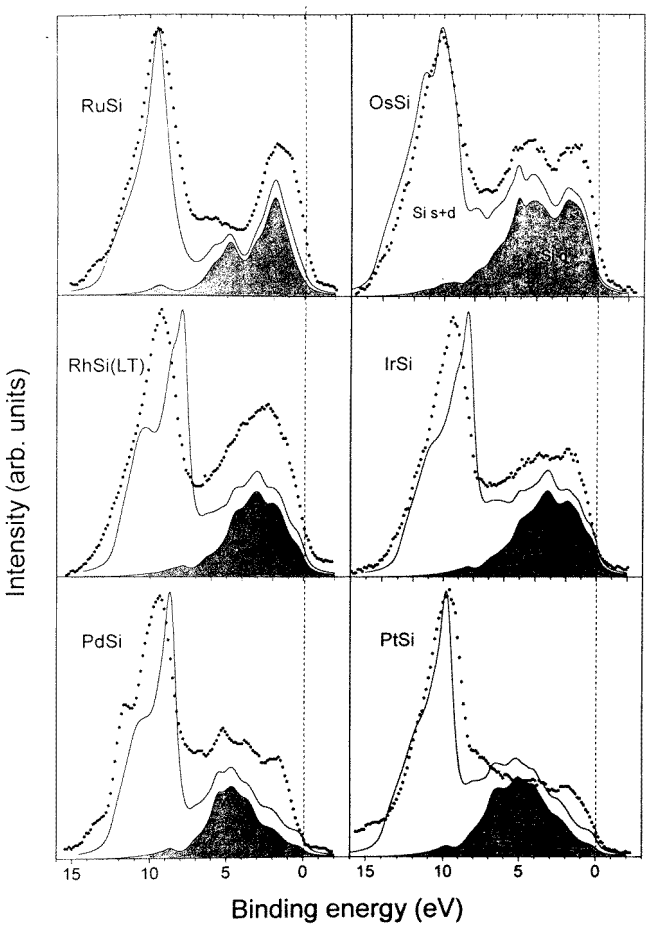

Figure 6. Comparison of Si $L_{2,3}$ XES and Si 3s3d DOS of 4d and 5d silicides.

The general trends in transition metal silicide bonding [18, 19] can be classified as follows.

(i) Transition metal d bands dominate the DOS and have increased binding energy with increasing Z. This energy shift is found to be relatively small when the d band density of states is high at E_f and larger when the d band is almost filled.

(ii) As the atomic number of the d metal is increased, the centre of gravity of the Si 3p states moves to the higher binding energy following the corresponding shift of d-metal states. This observation is connected with hybridization of silicon 3p orbitals with transition metal d states.

(iii) The Si 3s-derived states overlap relatively little with Si 3p or *n*d-metal states and these states are not important in bonding.

(iv) Various authors emphasize that the majority of the transition metal d states form a dominant non-bonding d state between the bonding and antibonding *n*d–Si 3p bonds which is considered a characteristic feature of silicide formation.

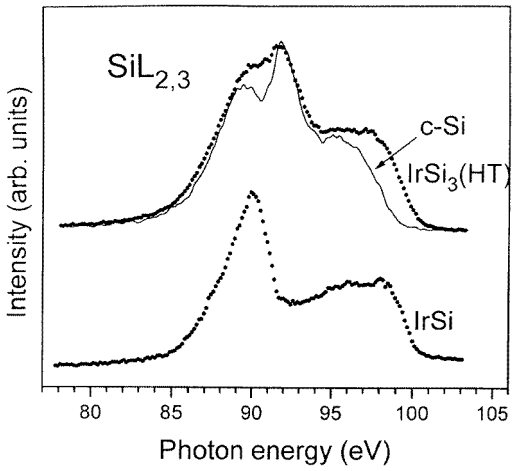

Figure 7. Si $L_{2,3}$ XES of Ir silicides and c-Si.

The results obtained in the present paper for 4d and 5d silicides generally confirm conclusions (i)–(iii) stated above. A shift of the d band to the higher binding energies is observed as Z increases as well as hybridization between silicon 3p and transition metal d states. The Si 3s states according to LMTO band structure calculations do not mix with Si 3p and transition metal nd states.

On the other hand, conclusion (iv) about the non-bonding character of the majority of nd states seems to be incorrect for 4d and 5d silicides. According to our XPS and XES measurements nd states are strongly hybridized with Si 3p states over the whole valence band. In addition we have obtained new evidence of the participation in chemical bonding of Si 3d states which are hybridized with transition metal nd states.

4. Conclusion

A fairly complete study of the electronic structure of 4d and 5d silicides (RuSi, RhSi, PdSi, OsSi, $IrSi_3$, Ir_3Si_5, IrSi, PtSi) has been undertaken which included XPS VB and XES (Si $K\beta_{1,3}$ and Si $L_{2,3}$) measurements and LMTO–ASA band structure calculations. We found that the d bands dominate the DOS and are more localized with increasing Z. Measurements and calculation provide evidence for strong hybridization between silicon 3p and the transition metal nd states over a large part of the valence band. Si 3s states are found to be not mixed with Si 3p and nd states; however, Si 3d states participate in bonding and hybridize with nd states of the metallic atoms and lead one to the conclusion that the majority of nd states are bonding states for 4d and 5d silicides.

Acknowledgments

This work was supported by the RFFI-INTAS programme (project 95-IN-RU-565), the Russian Foundation for Basic Research (projects N 96-03-3209 and 96-5-96598), a NATO Linkage Grant, NSF grant DMR-9017997 and a DOE-EPSCOR research grant DOE-LEQSF (1993-95)-03.

References

[1] Kurmaev E Z, Shamin S N, Galakhov V R, Wiech G, Majkova E and Luby S 1995 *J. Mater. Res.* **10** 907
[2] Nakamura H, Iwami M, Hirai M, Kusaka M, Akao F and Watabe H 1990 *Phys. Rev.* B **41** 12 092
[3] Weijs P J W, van Leuken H, de Groot R A, Fuggle J C, Reiter S, Wiech G and Buschow K H J 1991 *Phys. Rev.* B **44** 8195
[4] Kurmaev E Z, Fedorenko V V, Shamin S N, Postnikov A V, Wiech G and Kim Y 1992 *Phys. Scr.* **41** 288
[5] Galakhov V R, Kurmaev E Z, Cherkashenko V M, Yarmoshenko Yu M, Shamin S N, Postnikov A V, Uhlenbrock St, Neumann M, Lu Z W, Klein B M and Shi Zhu-Pei 1995 *J. Phys.: Condens. Matter* **7** 5529
[6] Simünek A, Polcik M and Wiech G 1995 *Phys. Rev.* B **52** 11 865
[7] Jia J J, Callcott T A, O'Brien W L, Dong Q Y, Rubensson J E, Mueller D R, Ederer D L and Rowe J E 1991 *Phys. Rev.* B **43** 4863
Jia J J, Callcott T A, Asfaw A, Carlisle J A, Terminello L J, Ederer D L, Himpsel F J and Perera R C C 1995 *Phys. Rev.* B **52** 4904
[8] Speier W, Kumar L, Sarma D D, de Groot R A and Fuggle J C 1989 *J. Phys.: Condens. Matter* **1** 9117
[9] Yamauchi S, Kawamoto S, Hirai M, Kusaka M, Iwami M, Nakamura N, Ohshima H and Hattori T 1994 *Phys. Rev.* B **50** 11 564
[10] Didyk V V, Zakharov A I, Krivitskii V P, Narmonev A G, Senkevich A and Yupko L M 1982 *Izv. Akad. Nauk USSR, Ser. Fiz.* **46** 802
Grunthaner P J, Grunthaner F J and Madhukar A 1982 *J. Vac. Sci. Technol.* **20** 680
[11] Wittmer M, Oelhafen P and Tu K N, 1986 *Phys. Rev.* B **33** 5
[12] Göransson K, Engström I and Noläng B 1995 *J. Alloys Compounds* **219** 107
[13] Andersen O K 1975 *Phys. Rev.* B **12** 3060
[14] Skriver H L 1984 *The LMTO Method* (Berlin: Springer)
[15] von Barth U and Hedin L 1972 *J. Phys. C: Solid State Phys.* **5** 1629
[16] Yeh J J and Lindau I 1985 *At. Data Nucl. Data Tables* **32** 1
[17] Kurmaev E Z, Galakhov V R, Shamin S N, Rodriguez T, Almendra A, Sanz-Maudes J and Göransson K 1997 *J. Mater. Res.* submitted
[18] Weaver J H, Franciosi A and Moruzzi V L 1984 *Phys. Rev.* B **29** 3293
[19] Pettifor D and Podloucky R 1986 *J. Phys. C: Solid State Phys.* **19** 315
[20] Engström I and Johnsson T 1987 *Acta Chem. Scand.* A **41** 237
[21] Engström I 1970 *Acta Chem. Scand.* **24** 1466
[22] Graeber E J, Baugham R J and Morosin B 1973 *Acta Crystallogr.* B **29** 1991
[23] Engström I, Lindsten T and Zdansky E 1987 *Acta Chem. Scand.* A **41** 237
[24] White J G and Hockings E F 1971 *Inorg. Chem.* **10** 1934
[25] No UPS Ir 5d shift with Ir content for Ir silicide thin films prepared by coevaporating irridium and silicon was found in [11]. Most probably the cleaning procedure of the samples (by 1000 eV Ar^+ sputtering for 30 min) used in these measurements was accompanied by redistribution of Ir and Si content in silicides.